

SUPPLEMENTAL MATERIALS

ASCE Journal of Hydrologic Engineering

Quantifying the Impact of Climate Change on Peak Stream Discharge for Watersheds of Varying Sizes in the Coastal Plain of Virginia

Mohamed M. Morsy, Binata Roy, Yawen Shen, Jeffrey M. Sadler,
Alexander B. Chen, Faria T. Zahura, and Jonathan L. Goodall

DOI: 10.1061/JHYEFF.HEENG-6114

© ASCE 2024

www.ascelibrary.org

Table S1. Selected NOAA weather stations for the IDF curve development. Bold font indicates a station used to create precipitation inputs for the 2D hydrodynamic TUFLOW model.

No.	Station ID	Station Name	Latitude	Longitude	Elevation (m)	Start	End	Record Length (years)
1	USC00441136	Buckingham	37.5083	-78.5333	176.8	1894	2019	125
2	USC00441209	Burkes Garden	37.0908	-81.33639	935.1	1896	2019	123
3	USC00441593	Charlottesville 2 W	38.0329	-78.5226	264	1892	2019	127
4	USC00441614	Chatham	36.8224	-79.4104	198.4	1922	2019	97
5	USC00441955	Concord 4 SSW	37.2819	-78.9591	248.4	1950	2019	69
6	USC00441999	Copper Hill	37.08169	-80.13486	870.8	1940	2019	79
7	USC00442208	Dale Enterprise	38.4547	-78.9352	413.9	1892	2019	127
8	USC00442790	Emporia 1 WNW	36.6983	-77.5597	30.5	1892	2019	127
9	USC00442941	Farmville 2 N	37.3263	-78.3864	137.2	1897	2019	122
10	USC00444044	Holland 1 E	36.683	-76.7684	24.4	1933	2018	85
11	USC00444101	Hopewell	37.2992	-77.2775	12.2	1916	2019	103
12	USC00444148	Huddleston 4 SW	37.12587	-79.5251	273.4	1950	2019	69
13	USC00444414	John H Kerr Dam	36.6002	-78.3011	76.2	1948	2019	71
14	USC00444876	Lexington	37.7767	-79.4385	334.4	1889	2019	130
15	USC00445050	Louisa	38.0421	-78.0061	128	1916	2019	103
16	USC00445096	Luray 5 E	38.6661	-78.3727	426.7	1941	2019	78
17	USC00445851	Mount Weather	39.0643	-77.8883	505.7	1914	2017	103
18	USC00446712	Piedmont Research Station	38.2323	-78.1202	158.5	1946	2019	73
19	USC00448192	Suffolk Lake Kilby	36.7297	-76.6015	6.7	1945	2019	74
20	USC00448737	Vienna	38.8922	-77.2892	127.4	1925	2019	94
21	USC00448829	Walkerton 2 NW	37.7434	-77.04	15.2	1932	2019	87
22	USC00448894	Warsaw 2 NW	37.9881	-76.7769	42.7	1892	2019	127
23	USC00449151	Williamsburg 2 N	37.3017	-76.7039	21.3	1948	2019	71
24	USC00449263	Woodstock 2 NE	38.8969	-78.4679	205.7	1889	2019	130
25	USC00449301	Wytheville	36.9617	-81.087	749.2	1892	2019	127
26	USW00013733	Lynchburg International Airport	37.3208	-79.2067	286.5	1944	2019	75
27	USW00013737	Norfolk International Airport	36.9033	-76.1922	9.1	1945	2019	74
28	USW00013740	Richmond International Airport	37.51151	-77.32344	50	1939	2019	80
29	USW00013741	Roanoke International Airport	37.3169	-79.9741	358.1	1947	2019	72

Table S2. Combinations of twenty-eight future IDF scenarios for seven return periods under two RCP scenarios on two target years (mid-century and end of the century).

Combinations	RCP_Time_Return period	Combinations	RCP_Time_Return period
S1	RCP4.5_2045_1	S15	RCP8.5_2045_1
S2	RCP4.5_2045_2	S16	RCP8.5_2045_2
S3	RCP4.5_2045_5	S17	RCP8.5_2045_5
S4	RCP4.5_2045_10	S18	RCP8.5_2045_10
S5	RCP4.5_2045_25	S19	RCP8.5_2045_25
S6	RCP4.5_2045_50	S20	RCP8.5_2045_50
S7	RCP4.5_2045_100	S21	RCP8.5_2045_100
S8	RCP4.5_2085_1	S22	RCP8.5_2085_1
S9	RCP4.5_2085_2	S23	RCP8.5_2085_2
S10	RCP4.5_2085_5	S24	RCP8.5_2085_5
S11	RCP4.5_2085_10	S25	RCP8.5_2085_10
S12	RCP4.5_2085_25	S26	RCP8.5_2085_25
S13	RCP4.5_2085_50	S27	RCP8.5_2085_50
S14	RCP4.5_2085_100	S28	RCP8.5_2085_100

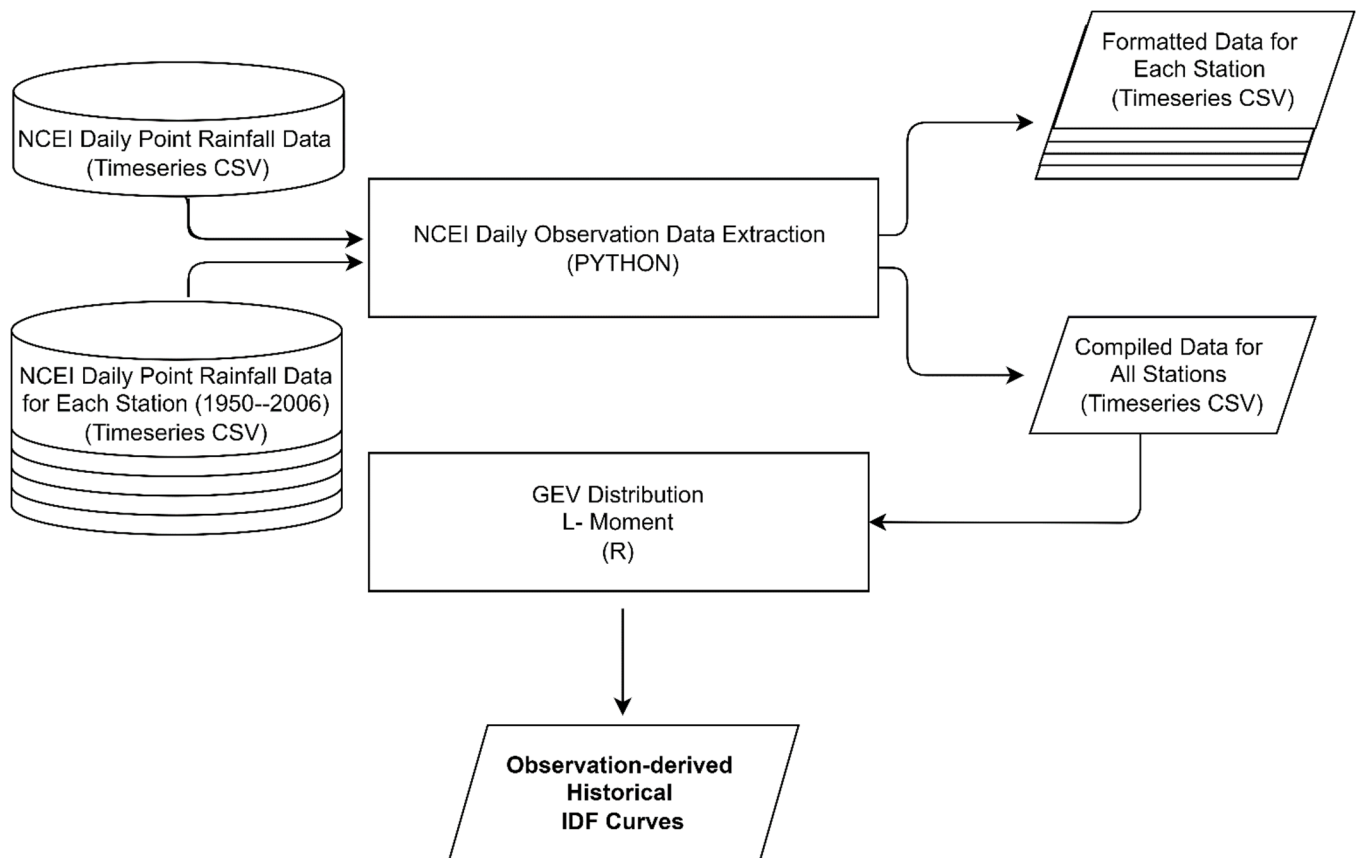


Fig. S1. Workflow for producing observation-derived historical IDF curves from historical data. Analysis steps are shown as rectangles, key input datasets are shown as cylinders, key result datasets are shown as parallelograms and final result is shown as parallelograms with bold font.

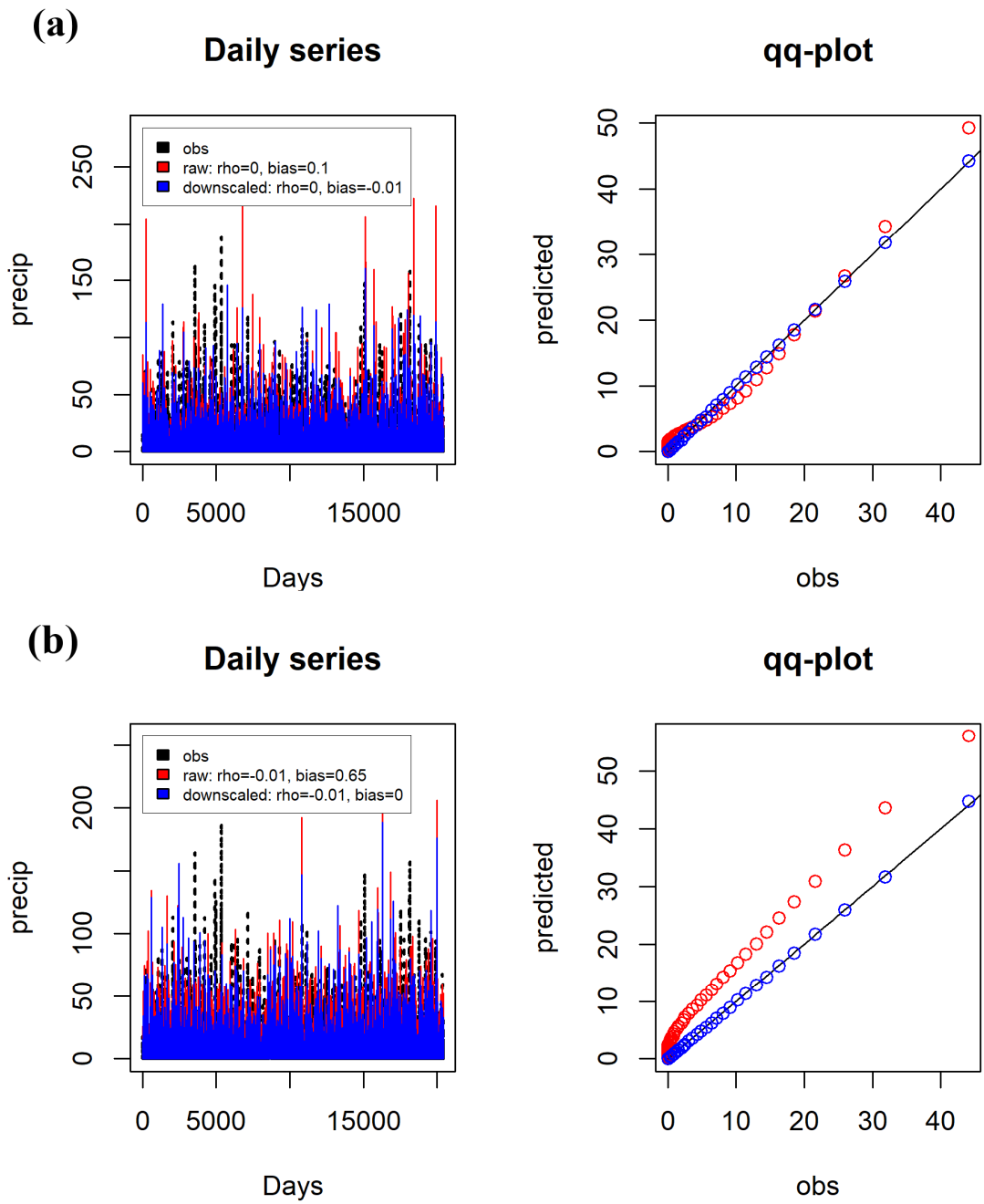


Fig. S2: Bias correction using a Q-Q Plot method for (a) CanESM2_CanRCM4 and (b) CanESM2_CRCM5-UQAM. The red is the original model output, and the blue is the bias-corrected model output.

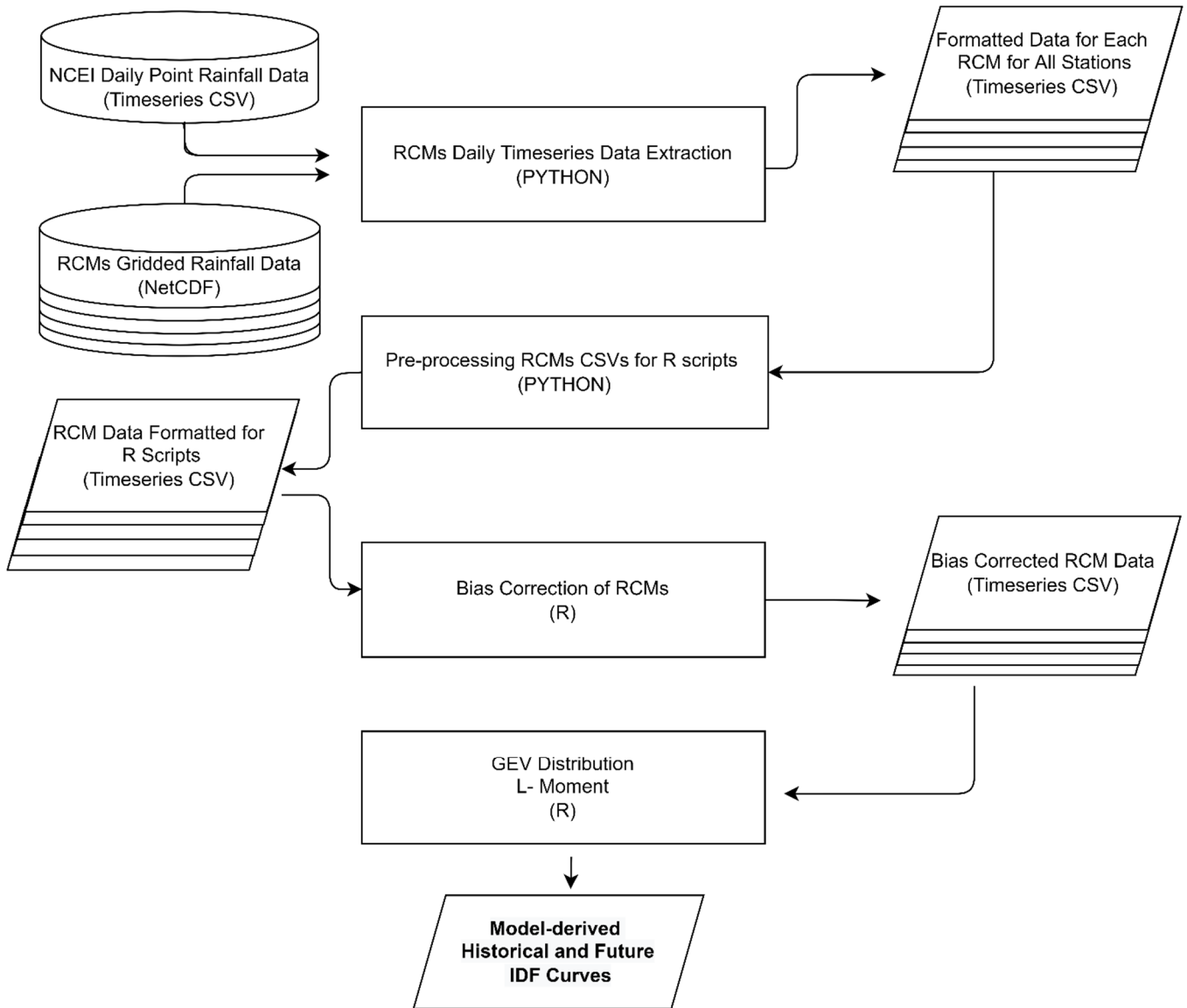


Fig. S3. Workflow for producing model-derived historical and future IDF curves from RCMs data. Analysis steps are shown as rectangles, key input datasets are shown as cylinders, key result datasets are shown as parallelograms and final result is shown as parallelograms with bold font.

G

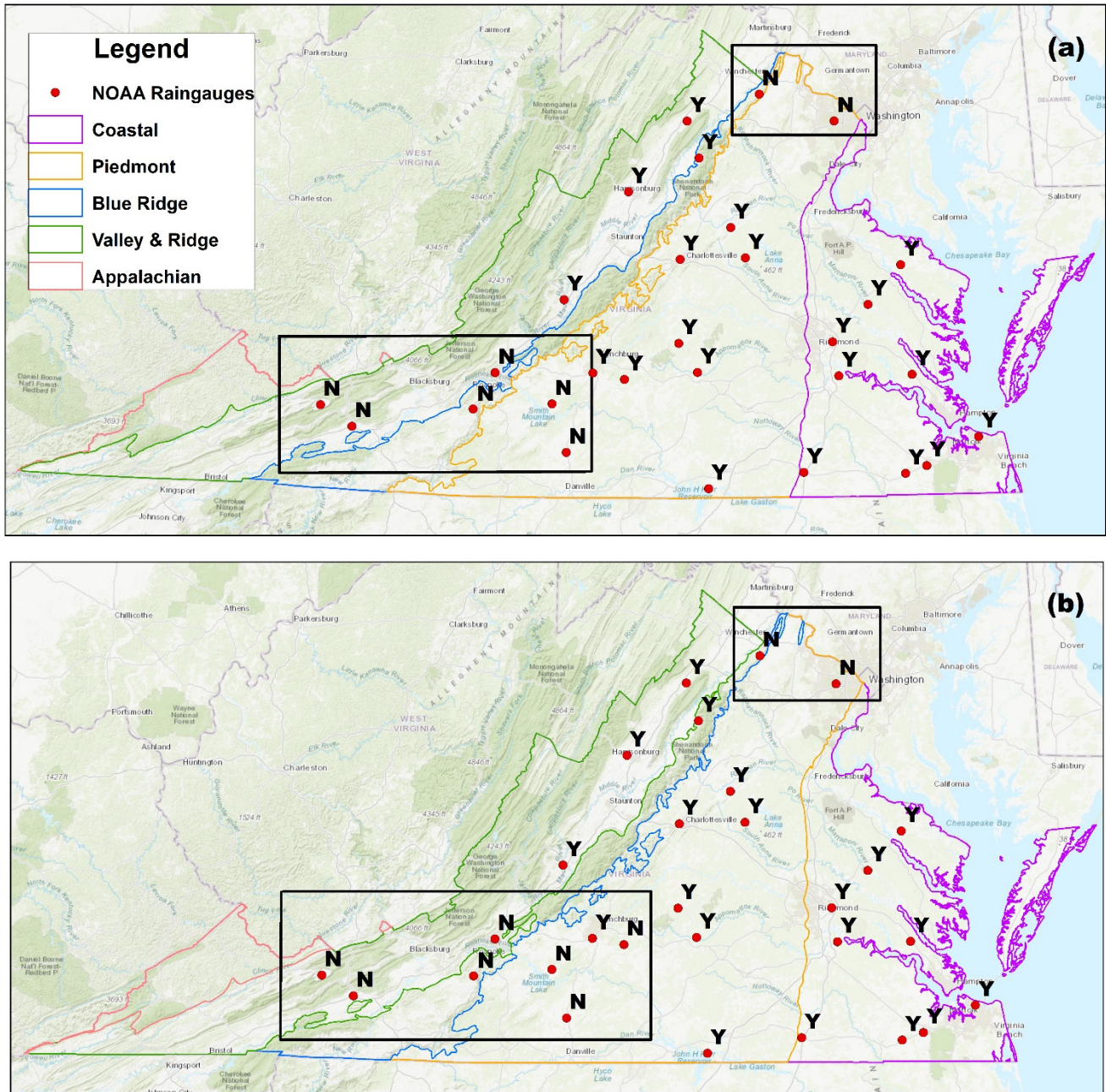


Fig. S4: The comparison between the increase in (a) precipitation (mm) and (b) precipitation (%) for RCP4.5 and RCP8.5. Here, ‘Y’ denotes ‘RCP8.5>RCP4.5’, and ‘N’ donates ‘RCP4.5>RCP8.5’. (Base map from ArcGIS World Topographic Map, Sources: Esri, HERE, Garmin, Intermap, INCREMENT P, GEBCO, USGS, FAO, NPS, NRCAN, GeoBase, IGN, Kadaster NL, Ordnance Survey, Esri Japan, METI, Esri China (Hong Kong), © OpenStreetMap contributors, GIS User Community.)

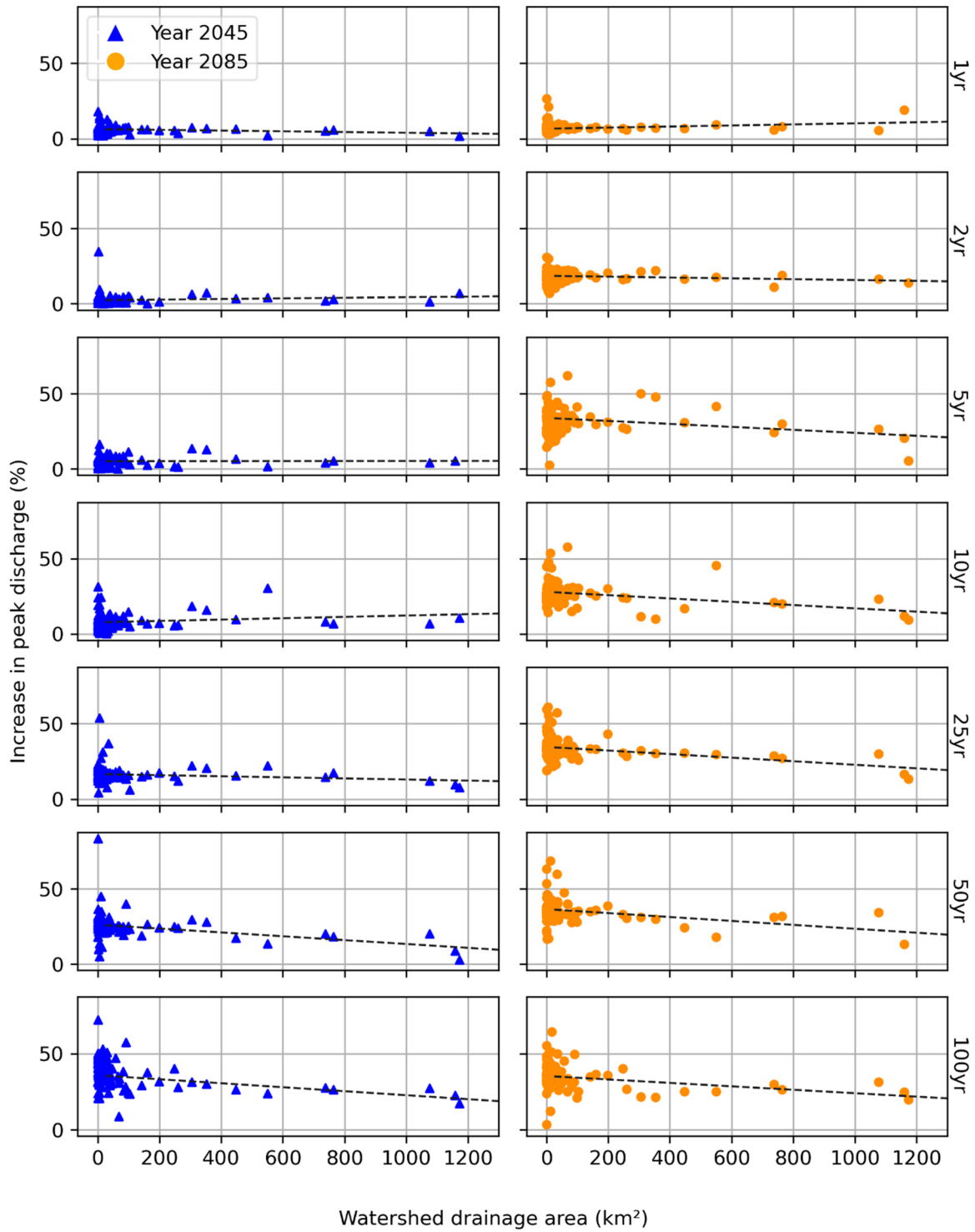


Fig. S5. Percent increase of peak discharge for design storms versus watershed drainage area under RCP4.5. Trendline is for watersheds with drainage area $> 25 \text{ km}^2$.

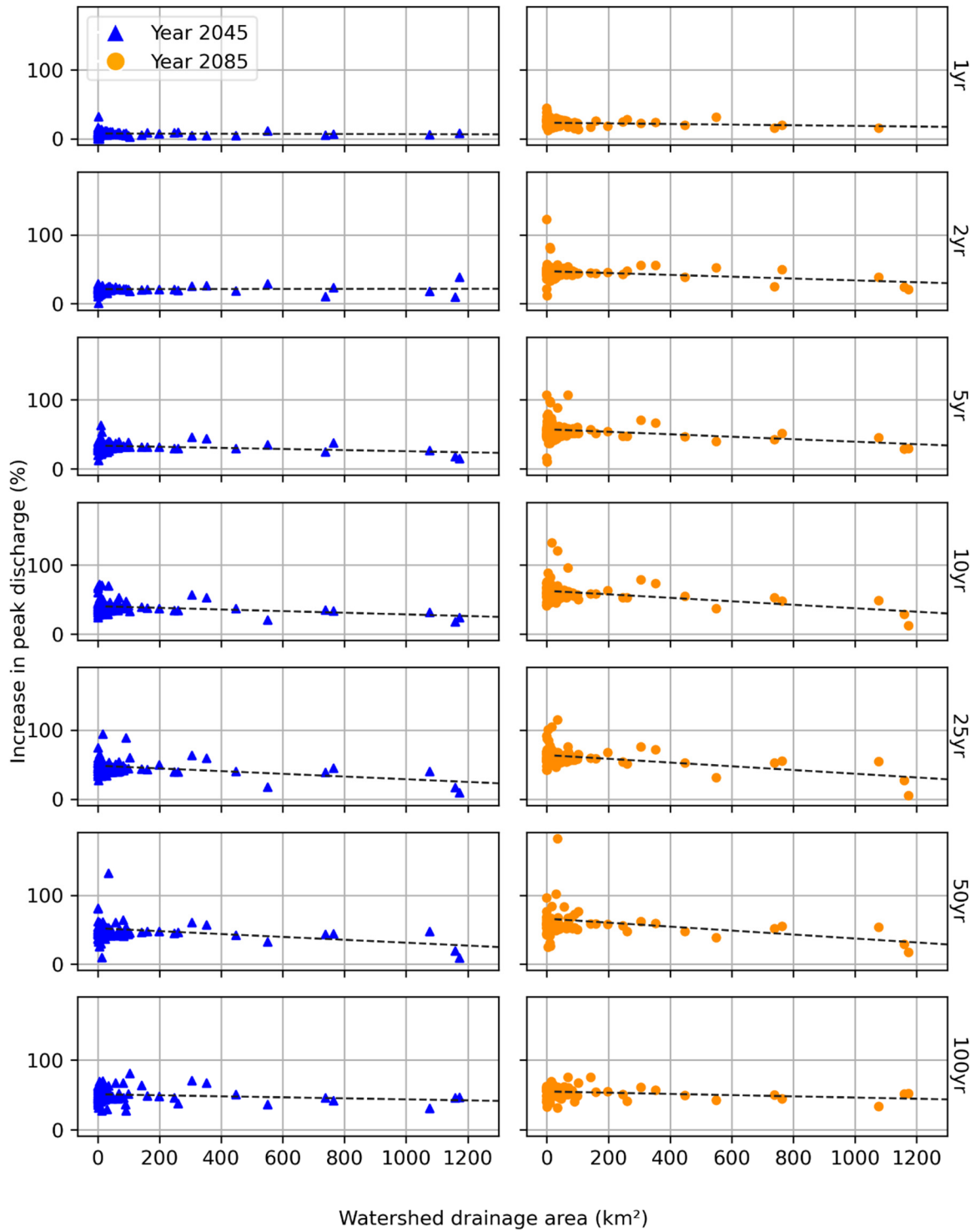


Fig. S6. Percent increase of peak discharge for design storms versus watershed drainage area under RCP8.5. Trendline is for watersheds with drainage area $> 25 \text{ km}^2$.